A Novel Underactuated Wire-Driven Robot Fish with Vector Propulsion

Zheng Li, *Student Member IEEE, ASME* Yong Zhong and Ruxu Du, Fellow, *ASME, SME, HKIE*

Abstract— **This paper presents a novel robot fish with vector propulsion. It can swim like a shark and/or a dolphin. The propulsor (tail) of the robot has an underactuated serpentine backbone and the actuation is done by two sets of orthogonally distributed wires. The backbone is composed of seven vertebras and an elastic rod. The vertebras are articulated by the rod and spherical joints. The horizontal flapping and vertical flapping are independently actuated by two motors. This enables the propulsor providing thrust in all directions. Propulsion model of the propulsor is developed by integrating the kinematic model and Lighthill's elongated body theory. A prototype is built. Tests show that the robot fish could flap its tail like the shark or the dolphin effectively. In the swimming tests, the maximum swimming speed of the robot is 0.35 BL/s.**

I. Introduction

With the increasing interest of ocean exploration and water quality monitoring, under water vehicle (UWV) has been a hot topic in recent years [1]. Among all the UWVs, the robot fish is the favorite choice. Inspired by fish, it is propelled by the caudal fin [2] or pectoral fins [3]. Compared with UWVs driven by screw propellers, the robot fish is believed to be efficient, agile and quiet. In nature, fish's propulsion efficiency can exceed 90% [4], and the acceleration can be 244.9 m/s^2, which is over 25g [5]. The flapping speed of the fin is much smaller than that of the screw propeller. This muffles the acoustic noise. The outstanding performance of fish can not be achieved without its propulsion system – the fins. There are two types of fish actuations, i.e. body and/or caudal fin (BCF) and medium and/or paired fin (MPF) [6]. It is estimated that over 85% of fish swim in BCF mode. The BCF motion can be roughly categorized as oscillatory form (e.g. carp), and undulatory form (e.g. eel). Most fast swimming fish, such as pike, tuna, and sailfish swim in oscillatory form. As a result, oscillatory caudal fin is the most frequently chosen option when people building robot fishes.

The fish body is flexible and can actively bend. To imitate the body motion, there are a couple of methods. One method is to use mechanisms, e.g. crank, four bar mechanism, eccentric wheel, etc. These mechanisms can transform motor rotation to back and forth motion. The flapping motion is achieved by swinging the tail using this back and forth motion. Flapping the tail by this method is simple, easy to control and the flapping force is large. However, the flapping motion is stiff, which is more like a paddle. Also, the efficiency is reduced a lot. Passive flexible fins may connect to the tail. This can improve the efficiency, but the effect is limited [7]. Another way is by controlling the motion of a chained rigid links [8]. Each link is actuated by a motor. The fish body curve is fitted by the rigid serpentine structure, or a polyline. Typically, the number of links is below six. With increased segments, the fish body can be better mimicked. However, the structure as well as control of the robot becomes more complicated. With the development of smart materials, people have been trying to replace the motors by these materials, such as Shape Memory Alloy (SMA) [9] and Electro Active Polymer (EAP), typically Ionic Polymer Metal Composite (IPMC) [10]. These materials are flexible, and the shape can be actively controlled. Compared with traditional motor-based methods, in this method the fish body curve is better mimicked. However, deficiencies also exist. SMA is controlled by temperature, which limits the flapping frequency of the propulsor. IPMC is soft and the flapping force is low. Also, due to the nonlinear properties, such as hysteretic, the flapping motion of smart material propulsors is difficult to control.

A close examination of fish anatomy reveals that the fish backbone is composed of a serial of chained vertebras. When swimming, the joints' rotations are more or less the same. This inspired employing the biomimetic wire-driven mechanism [11]. Flapping propulsors and robot arms / fishes have been built based on this mechanism [12-14]. The underactuated design reduces the number of actuators, while the flexible backbone fits the fish body curve well. It adopts a motor as actuator, which can provide large flapping force and simplifies the control. To the best of our knowledge, existing oscillatory flapping propulsors all flap in horizontal plane like the shark [7-10], or in vertical plane like the dolphin [15, 16]. Apparently, both types of flapping are effective in propelling the animal. Nonetheless, the differences are obvious. The shark-like flapping can provide thrust in the horizontal plane, while the thrust provided by the dolphin-like flapping is within the vertical plane. As a result, the dolphin excels in leaping out of the water, while the shark is cruising in water most of the time. It would be interesting to integrate these two types of flapping motion together. With adjustable horizontal and vertical component, the propulsion magnitude and direction can be controlled. Driven by the vector propulsor, the robot fish is predicted to turn to any chosen direction using the tail only. This will enhance the robot's maneuverability.

In this paper, we designed a flapping propulsor that can flap horizontally and vertically independently. It is based on the biomimetic wire-driven mechanism. The idea was validated by a robot fish prototype. The rest of the paper is organized as follows: Section 2 presents the robot fish design; Section 3 derives the propulsion model based on Lighthill's

Zheng Li is with the Institute of Precision Engineering, Department of Mechanical & Automation Engineering, the Chinese University of Hong Kong, Hong Kong, China (phone: 852-3943-4237; fax: 852-2603-6002; email: zli@mae.cuhk.edu.hk).

Yong Zhong is with the Guangzhou Institute of Advanced Technology, Guangzhou, China (email: yong.zhong@siat.ac.cn).

Ruxu Du is with the Institute of Precision Engineering, Department of Mechanical & Automation Engineering, the Chinese University of Hong Kong, Hong Kong, China (email: rdu@mae.cuhk.edu.hk).

theory; Section 4 presents the robot fish prototype; Section 5 presents the experiment results; Section 6 concludes the paper.

II. ROBOT FISH DESIGN

The robot fish is composed of the vector propulsor and the fish body. The propulsor provides thrust with controllable direction, and the fish body houses the actuator, controller, power, etc. Their designs are described as follows:

A. Vector Propulsor Design

Direction of the thrust generated by the propulsor is in the flapping plane. Existing oscillatory flapping propulsors can only flap in the horizontal plane or the vertical plane. As a result, if actuated by the tail solely, the robot fish can only move in horizontal plane, i.e. forward and turn left or right, or in vertical plane, i.e. forward and turn upward or downward. In this design, the tail can independently flap horizontally and vertically. Figure 1 (a) shows the designed propulsor. It is composed of the tail base, several vertebras, fins, elastic rod and the controlling wires. Four fin pieces are inserted to the last vertebra as shown in the figure. Two opposite fin pieces form a crescent caudal fin. The vertebra is shown in Figure 1(b). It has four orthogonally distributed ribs. A wire eyelet penetrates each rib. On the front of the vertebra there is a convex spherical surface, and on the back of the vertebra there is a concave spherical surface with the same diameter. In the middle of the vertebra is a central cavity, which connects to the elastic rod. The number of vertebras can be a lot. Seven vertebras are shown in the figure. Two adjacent vertebras form a spherical joint. The vertebras are articulated by a uniform elastic rod as well as the joint. The rod confines the vertebra from rotating about its own axis, as a result the joint can only rotate about the X axis and the Y axis, i.e. the propulsor can bend horizontally and vertically without twisting. The rotations are controlled by two sets of wires, which are guided by the eyelets on the vertebra rib as shown in Figure 1(b). As the two sets of wires are orthogonally arranged the horizontal rotation and vertical rotation are independent. The wires work in pairs. By pulling one wire and unwinding the other wire, the propulsor bends to the pulled wire. The load acted on the elastic rod is a pure moment, ideally it will deform to a circular arc. Therefore, all the joint rotations are the same during the propulsor flapping.

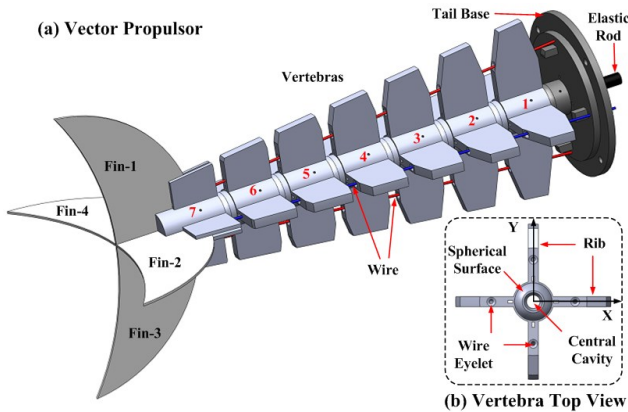**(a) Vector Propulsor**

(b) Vertebra Top View

Figure 1. Vector Propulsor Design: (a) Vector Propulsor Isometric View; (b) Vertebra Top View

Figure 2 shows the cross section view of the joint. The wire pilot hole is tilted with respect to the propulsor axis,

which is helpful in reducing the wire tension [14]. In the figure, H is the rib height; h_0 is the joint gap distance; r_1 is the top wire eyelet central distance; R_1 is the vertebra top width; r_2 is the bottom eyelet central distance; R_2 is the vertebra bottom width; R is the radius of the stopper. The joint can independently rotate about the X axis and the Y axis, and the two rotations are identical. The maximum joint rotation angle is determined by the joint gap distance h_0 and the stopper radius R as shown in Figure 2(b). Their relationship is:

$$\theta_{max} = 2\arctan\left(\frac{h_0}{2R}\right) \qquad (1)$$

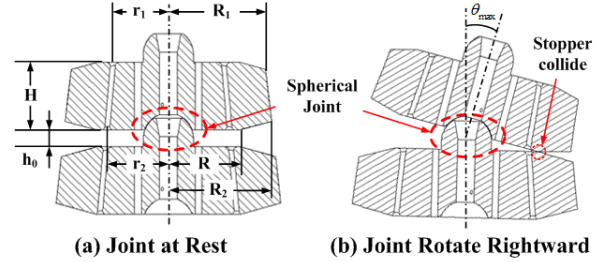**(a) Joint at Rest**   **(b) Joint Rotate Rightward**

Figure 2. Joint Rotation: (a) Joint at rest; (b) joint rotate rightward

In the designed vector propulsor, there are seven vertebras. The sizes of the vertebras are as shown in table I, and the unit is mm. Each joint could rotate up to 13.5° in the X and Y direction. The maximum bending angle of the tail is 94.5°.

TABLE I.   VERTEBRA PARAMETERS (IN MM)

Num	H	h_0	R	R_1	R_2	r_1	r_2
1	20	5	21.12	20.00	22.29	10.00	11.71
2	20	5	21.12	22.86	25.14	12.14	13.86
3	20	5	21.12	25.71	28.00	14.29	16.00
4	20	5	21.12	28.57	30.86	16.43	18.14
5	20	5	21.12	31.43	33.71	18.57	20.29
6	20	5	21.12	34.29	36.57	20.71	22.43
7	20	5	21.12	37.14	39.43	22.86	24.57

B. Fish Body Design

Figure 3 shows the robot fish body design. The fish body is composed of the hull, main board, auxiliary board, servo motors, wire coilers, controller, battery, pulleys etc. The hull has three pieces: hull-1, hull-2 and hull-3. Hull-1 is the base of the robot fish. The main board and tail base are fastened to Hull-1. Hull-2 is positioned to Hull-1 by four pegs. It is used to facilitate the robot fish assembly. Hull-3 has a parabolic front surface, which is helpful in reducing the water resistance. The assembly procedure is also shown in the figure: Step I, connect Hull-2 to Hull-1; step II, cover the fish body by Hull-3. The three pieces form a cylindrical robot fish hull.

Two servo motors are used to control the wire lengths. The motor in front controls the vertical wire group, while the other one controls the horizontal wire group. The wires are guided by the pulleys. One end of the wire is fixed at the last vertebra, and the other end is connected to the wire coiler, which rotates with the servo motor. The motor motion is controlled by the MCU controller. The control scheme is similar to [13]. The command is send out by the operator using a remote controller or using comport via Bluetooth. On receiving the signal, the

MCU generates a 50Hz PWM (Pulse Width Modulation) sequence. The position of the servo motor is controlled by the duty cycle of the PWM, while the velocity is controlled by setting the time delays between positions.
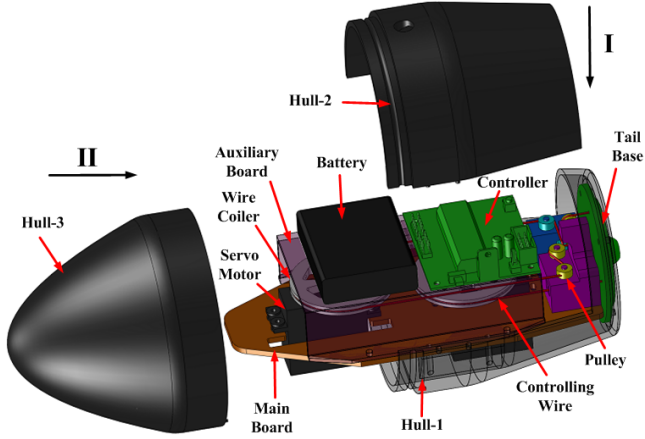

Figure 3.   Fish body design

C. Robot Fish Prototype

The robot fish prototype is built as shown in Figure 4. In the prototype there are 7 vertebras, which are made by rapid prototyping. The size of each vertebra is as listed in table 1. The maximum rotation of each joint is 13.5^{o}. The vertebras are connected by a silicon rubber rod with a diameter of 5mm. To improve the elasticity, four carbon sticks with 0.5mm diameter are connected to the tail. To reduce the friction, lubricating grease is added to all the joints. Four plastic fins are orthogonally mounted to the last vertebra. Two opposite fins make a lunate shape, which is similar to the caudal fin of the dolphin. Two servo motors are used to control the propulsor bending. The length of the robot fish is 425mm. The overall weight of the robot fish is 1.65kg. Figure 4(b) shows the fish tail bending in horizontal plane. In this mode, the bending is controlled by the horizontal wire group, and the vertical wire group remains still. Figure 4(c) shows the fish tail bending in the vertical plane. In this mode, the tail motion is controlled by the vertical wire group only. Figure 4(d) shows the robot fish tail bending in arbitrary direction. The bending magnitude and direction are controlled by the components in horizontal and vertical plane.
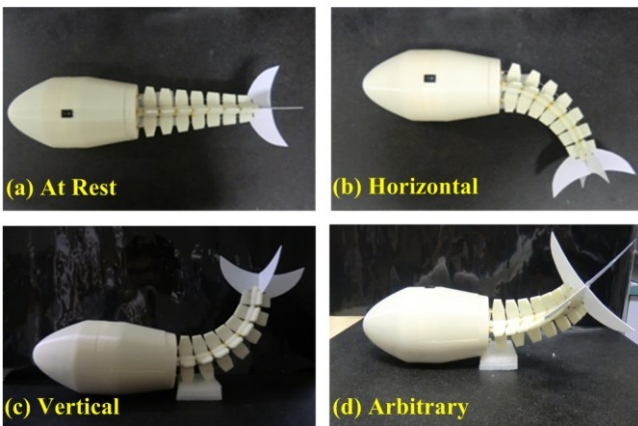

Figure 4.   Vector Propelled Robot fish Prototype: (a) robot fish in the rest position; (b) propulsor bending horizontally; (c) propulsor bending vertically; (d) propulsor bending in arbitrary direction

III. PROPULSION MODEL

Propulsion model of the vector propulsor is obtained by integrating the kinematic model into Lighthill's elongated body theory [17].

A. Kinematics Model

As shown in Figure 5, the configuration of the propulsor is determined by the flapping angle Θ and flapping direction Φ. The flapping angle is defined as the angle between the bended tail tip direction and the Z axis (tail tip direction at resting position). The flapping direction is defined as the angle between X axis (horizontal direction) and the flapping plane. The wire configuration is as shown in Figure 5(b), where $P1$, $P2$, $P3$, $P4$ denote the wire location. $P1$ and $P3$ are the horizontal wire group. They control the propulsor bend about Y axis (flap in horizontal plane). $P2$ and $P4$ are the vertical wire group. They control the propulsor bend about X axis (flap in vertical plane). When the flapping direction is Φ, it is conceived that the propulsor bends about a virtual axis Y' as shown in the figure. The distance from the wires in vertical group to the virtual axis is a, while the distance from the wires in horizontal group to the virtual axis is b.

(a) Tail Bending Illustration   **(b) Wire Configuration**
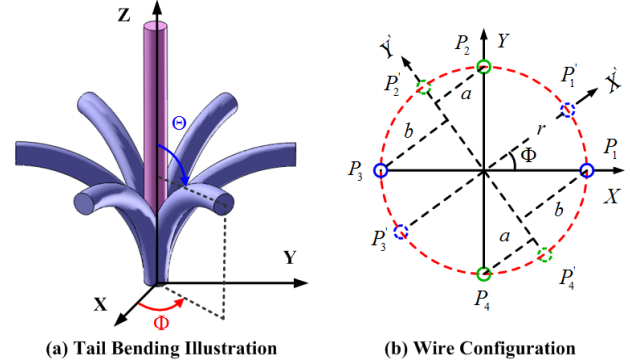
Figure 5.   Kinematics illustration

In this design, the joint rotations are confined by the elastic rod. As the vertebras are rigid, the backbone length is constant. The load acted on the propulsor is decoupled during wire pulling. The vertebras suffer the normal stress, while the rod suffers the bending moment only. Theoretically, the deformed shape of the rod under pure moment is a circular arc. Hence, we assume that all the joint rotations are the same during the flapping process. The relationships between the wire lengths and the propulsor configuration are as follows [11]:

$$P_1: \qquad L_1 = L_0 + 2N\left[b\cdot\sin\left(\frac{\theta}{2}\right) - h_0\cdot\sin^2\left(\frac{\theta}{4}\right)\right] \qquad (2)$$

$$P_2: \qquad L_2 = L_0 + 2N\left[a\cdot\sin\left(\frac{\theta}{2}\right) - h_0\cdot\sin^2\left(\frac{\theta}{4}\right)\right] \qquad (3)$$

$$P_3: \qquad L_3 = L_0 - 2N\left[b\cdot\sin\left(\frac{\theta}{2}\right) + h_0\cdot\sin^2\left(\frac{\theta}{4}\right)\right] \qquad (4)$$

$$P_4: \qquad L_4 = L_0 - 2N\left[a\cdot\sin\left(\frac{\theta}{2}\right) + h_0\cdot\sin^2\left(\frac{\theta}{4}\right)\right] \qquad (5)$$

where, $a = r\cdot\sin(\Phi)$ and $b = r\cdot\cos(\Phi)$; r is the mean of upper vertebra r_2 and lower vertebra r_1 (average distance between the

wire and Z axis); L_0 is the wire initial length; N is the number of vertebras; and $\theta = \Theta / N$ is the joint rotation.

From Equations (2)-(5), the flapping angle and direction can be represented as:

$$\Phi = \arctan\left(\frac{L_2 - L_4}{L_1 - L_3}\right) \tag{6}$$

$$\Theta = N \cdot \theta = 2N \cdot \arcsin\left[\frac{\sqrt{(L_1 - L_3)^2 + (L_2 - L_4)^2}}{4N \cdot r}\right] \tag{7}$$

The propulsor tip position with respect to the first joint rotate center is:

$$\begin{cases} x = \left\{(H_T - h_0/2) \cdot \sin(N \cdot \theta) + (H + h_0)\sum_{i=1}^{N} \sin[i \cdot \theta]\right\}\cos(\Phi) \\ y = \left\{(H_T - h_0/2) \cdot \sin(N \cdot \theta) + (H + h_0)\sum_{i=1}^{N} \sin[i \cdot \theta]\right\}\sin(\Phi) \\ z = (H_T - h_0/2) \cdot \cos(N \cdot \theta) + (H + h_0)\sum_{i=1}^{N} \cos[i \cdot \theta] \end{cases} \tag{8}$$

where, H is the rib height, h_0 is the joint initial gap distance and H_T is the fin length. The positions along the propulsor can be obtained accordingly. It is noted that the excursion of the propulsor tip from the Z axis is $\sqrt{x^2 + y^2}$. When all the joints rotate from one limit $\theta_{\min}$ to the other limit $\theta_{\max}$, the propulsor flaps from side to side. The flapping motion is in the plane defined by the flapping angle Φ, and the flapping motions in all planes are the same.

The fish body curve is viewed as a travelling wave. A well accepted fish swimming body curve model is shown in Equation (9). In this model, c_1 and c_2 are for the linear and quadratic body wave amplitude envelope, k is the body wave number and ω is the wave frequency [15]. Figure 6 shows the simulation of the fish body curve and the motion of the vector propulsor in the XZ plane. Parameters used in the simulation are: $c_1 = 0$, $c_2 = 4$, $k = 0.01$, and $\omega = \pi$. From the figure, it is seen that the propulsor motion matches the fish swimming body curve reasonably well.

$$x(z, t) = \left[c_1 z + c_2 z^2\right]\left[\sin(kz + \omega t)\right] \tag{9}$$

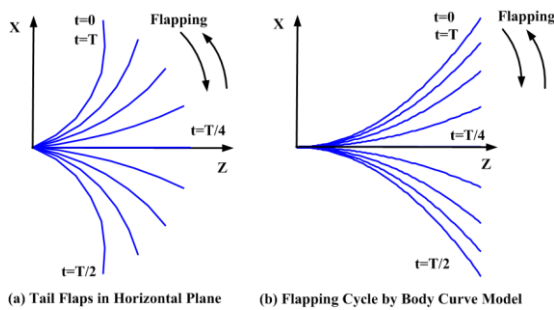(a) Tail Flaps in Horizontal Plane   (b) Flapping Cycle by Body Curve Model

Figure 6. Flapping cycle comparison: (a) Flapping cycle of the designed propulsor; (b) Flapping cycle by the fish body curve model

B. *Propulsion Model*

In the 1970's, James Lighthill proposed the large amplitude elongated body theory of fish locomotion, based on

which the propulsion model can be derived as shown in Equations (10)-(13) [4, 17, 18]. In the model, $q = L$ indicates the tip of the tail; U is the cruising speed; $m = 0.25\pi S_c^2 \rho\beta$ is the virtual mass density at the tip of the tail; ρ is the density of the water, β is a non-dimensional parameter close to 1; S_c is the width of the tail tip and $w(q, t)$ is the excursion of the tail. The cruising speed is obtained when the mean thrust ($\overline{T}$) equals the drag force (F_D). The Froude efficiency measure the portion of power used in propulsion.

Drag Force:
$$F_D = \frac{1}{2}C_D \rho U^2 S \tag{10}$$

Thrust:
$$\overline{T} = \left[\frac{m}{2}\left(\overline{\left(\frac{\partial w(q,t)}{\partial t}\right)^2} - U^2\overline{\left(\frac{\partial w(q,t)}{\partial q}\right)^2}\right)\right]\Bigg|_{q=L} \tag{11}$$

Cruise speed:
$$U = \left[\sqrt{\frac{m \cdot \overline{\left(\frac{\partial w(q,t)}{\partial t}\right)^2}}{C_D \rho S + m \cdot \left(\frac{\partial w(q,t)}{\partial q}\right)^2}}\right]\Bigg|_{q=L} \tag{12}$$

Froude efficiency:
$$\eta = \frac{U\overline{T}}{P} \times 100\% \tag{13}$$

From the kinematics model, the excursion, slope and the traversing speed of the propulsor are:

$$w(q,t)\big|_{q=L} = (H_T - h_0/2) \cdot \sin(N\theta) + (H + h_0)\sum_{i=1}^{N} \sin(i \cdot \theta) \tag{14}$$

$$\frac{\partial w(q,t)}{\partial q}\bigg|_{q=L} = \tan(\Theta) \tag{15}$$

$$\frac{\partial w(q,t)}{\partial t}\bigg|_{q=L} = \left\{(H_T - h_0/2) \cdot N \cdot \cos[N \cdot \theta] + (H + h_0)\sum_{i=1}^{N} i \cdot \cos[i \cdot \theta]\right\} \cdot \dot{\theta} \tag{16}$$

By substituting Equations (14)-(16) into Lighthill's large amplitude elongated body theory, the propulsion model of the vector propulsor is obtained.

IV. SWIMMING CONTROL

Figure 7 shows the control scheme of the robot fish. The command is sent to the Micro Control Unit (MCU) by the operator via a remote controller. On receiving the command, the MCU generates two channels of Pulse Width Modulation (PWM) sequences which control the velocity and position of the two servo motors. The motor rotate position and velocity is controlled by the pulse width. The rotations of the motors are transferred to the tail's flapping motion through the wire driven mechanism, and the robot fish is propelled by the vector thrust. The direction and magnitude of the thrust is controlled by the flapping motion. This is a human-in-loop control, with visual feedback established by the operator.
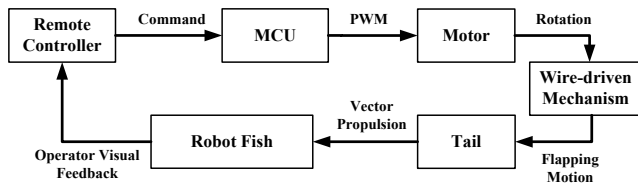
Figure 7. Robot Fish Swimming Control Scheme

The flapping cycle of the propulsor is divided into four stages. It is illustrated by the flapping in horizontal plane as shown in Figure 8. Stage I - Flap from resting position to the left limit; stage II - Flap from left limit back to the resting position; stage III - Flap from resting position to the right limit; stage IV - Flap from right limit back to the resting position. From the propulsion model, the thrust is affected by the flapping amplitude and frequency. By controlling the flapping amplitude and frequency in the four stages, the forward and turning speed is controlled. Similarly, the upward (diving) and downward (floating) speed of the robot fish is controlled by controlling the amplitude and frequency of the four stages in vertical flapping. When the propulsor flapping has both a X and Y component, turning in any chosen direction is possible. The direction is controlled by the magnitude of the two components.
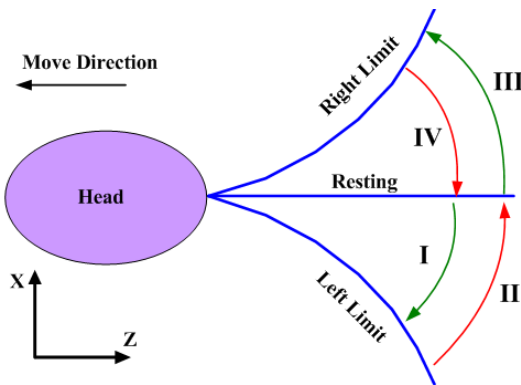

Figure 8. Flapping Cycle of the Propulsor

For the robot fish, there are three basic motion modes, i.e. moving forward, turning horizontally, turning vertically and turn in a chosen direction. In the forward mode, the propulsor flaps symmetrically. The flapping direction has no effect on the forward motion. In horizontal turning mode the propulsor flaps in the horizontal plane asymmetrically. When the propulsor flaps leftward more than flaps rightward, the robot fish turns to left, and vice versa. In the vertical turning mode the propulsor flaps in the vertical plane. When the propulsor flaps upward more than downward the robot fish turns upwards, and vice versa. For turning in a chosen direction, the approach is similar with turning horizontally or vertically. The difference is in the flapping plane direction.

V. SWIMMING EXPERIMENTS RESULTS

The robot fish is tested in an inflated swimming pool. The robot fish is covered with rubber skin to prevent water leakage. In the experiment, the robot fish swims in still water. Two basic swimming modes are presented here: swimming in shark form and swimming in dolphin form. For swimming using arbitrary directional flapping, the result is similar.

A. Swim in Shark Form

In this experiment, the vector propulsor flaps horizontally like a shark. In this mode, the back motor controls the horizontal wire group and the front motor keeps still. Fin 1 and fin 3 provide thrust, while fin 2 and fin 4 do not. The flapping frequency of the tail is f=1 Hz, and the flapping amplitude is 45 degree. At first, the robot fish is placed in the swimming pool. When the water is still, the robot fish is controlled via Bluetooth comport flapping horizontally. One flapping cycle is shown in Figure 9 (a)-(e). Figure 9 (a) shows the robot fish at resting position. Then, it flaps to the left as shown in Figure 9 (b). When it gets to the left most position, it flaps back to the resting position as shown in Figure 9 (c). The other half cycle is in a similar way. The propulsor flaps rightward at first, as shown in Figure 9 (d), and then flaps back to the resting position. In this experiment, the left flapping amplitude and right flapping amplitude are both 45 degree. Also, the flapping frequencies in the four stages are the same. From the results, it is shown that after one flapping cycle, the robot fish moves forward 148 mm, i.e. 0.35 BL. From the previous propulsion model, when the robot fish flapping frequency is 1 Hz, and the amplitude is 45 degree, i.e. the tail end excursion is 65 mm or 0.153 BL, the cruise speed of the robot fish is 170.4 mm/s. The prediction error is about 13%. In the simulation, the drag coefficient is selected as 0.5 [19].

B. Swim in Dolphin Form

In this experiment, the vector propulsor flaps vertically like a dolphin. Fin 2 and fin 4 provide thrust in this mode, while fin 1 and fin 3 do not. The flapping frequency of the propulsor is $f = 1$ Hz and the flapping amplitude is 45 degree. Same as the former test, the robot fish is placed in still water. When the fish received the command, it starts flapping vertically. In this mode, the front motor controls the vertical wire group and the back motor keeps still. Figure 9 (f)-(j) shows one flapping cycle. As shown in Figure 9 (f), the robot fish is at resting position, waiting for the command. On receiving the command, the tail flaps downward at first, as shown in Figure 9 (g). After reach the down-most position, the tail flaps back as shown in Figure 9 (h). The tail does not stop at resting position. It flaps until reach the upmost position as shown in Figure 9 (i). Finally, the tail flaps to the resting position and finishes a cycle. After a cycle, the tail does not stop. It keeps flapping and driven the robot fish moves forward. From the measurement, the distance the robot fish travels in one cycle is around 0.28 BL. The cruise prediction error for the dolphin form swimming is 30%. The error is larger than that in the previous case. One major reason is the flapping cycle is not fully occupied, i.e. part of the flapping is out of water.

C. Discussion

In the experiment, it is shown that the robot fish could swim effectively in both shark form and dolphin form. This validates the vector flapping propulsor design method. In both cases, the propulsion velocities are similar. Moreover, the velocity is close to the model prediction. The error sources include prototyping error, modeling error, measuring error, and etc. Although, the speed of dolphin form is less than that of shark form, it does not mean the shark form is superior. In fact, in the experiment, it is seen that in the dolphin form, the robot could employ the gravity to glide. In these preliminary

swimming tests the robot is not fully submerged in water. This limits the robot fish's 3D mobility performance. In the near future, the prototype will be fine-tuned and the 3D maneuverability (i.e. turning upward, downward, diving, surfacing) of the robot will be studied in detail.
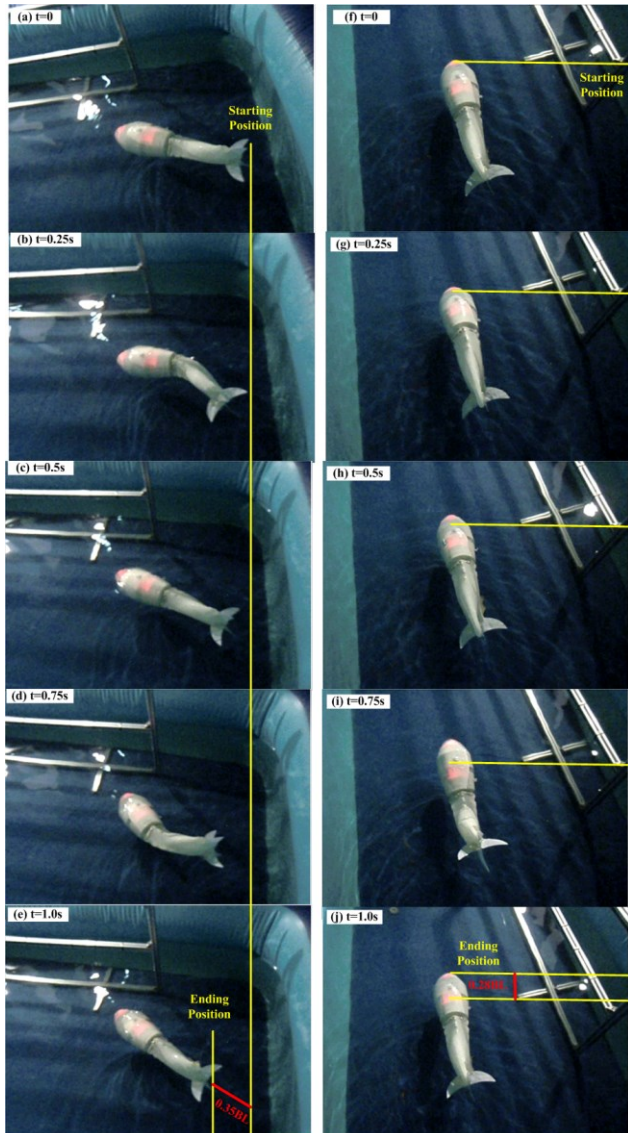

Figure 9.   Experiment Results: (a)-(e) is the flapping cycle of shark form swimming; (f)-(j) is the flapping cycle of dolphin form swimming

VI. CONCLUSION

This paper presents a novel underactuated wire-driven robot fish with vector propulsion. The robot fish propulsor is composed by a number of chained vertebras, a continuous elastic rod, four fins and two sets of controlling wires. The underactuated wire-driven design reduces the number of actuators, while preserving the propulsor motion resembling the fish swimming body curves. The propulsor can flap in both horizontal direction and vertical direction independently. This enables the propulsor flapping in any chosen direction, and providing vectored thrust. This can improve the robot's mobility. The kinematic model and propulsion model of the propulsor are developed. The design is validated by a robot fish. Propelled by the vector propulsor, the robot fish can swim like a shark or a dolphin effectively. Preliminary results show that the robot fish could swim up to 0.35 BL/s in the shark form and 0.28 BL/s in dolphin form. The prediction errors are 13% and 30% respectively. This is mainly due to the prototyping error and measurement error.

REFERENCES

[1]   SHOAL: http://www.roboshoal.com/
[2]   Triantafyllou, M. S. Triantafyllo, George S. "An efficient swimming machine", *Scientific American*, Vol. 271, Issue 3, Mar. 1995, pp. 64-70.
[3]   Yueri Cai, Shusheng Bi, et. al. "Design of a robotic fish propelled by oscillating flexible pectoral foils", *The 2009 IEEE/RSJ International Conference on Intelligent Robots and Systems*, Oct. 11-15, 2009, St. Louis, USA, pp.2138-2142.
[4]   M. J. Lighthill, "Aquatic animal propulsion of high hydro mechanical efficiency", *Journal of Fluid Mechanics*, Vol. 44, part 2, 1970, pp. 265-301.
[5]   John J. Videler, "Fish Swimming", *Fish kinematics: swimming movements stride by stride*, 1st ed., Vol. 10, Chapman & Hall Fish and Fisheries series, London, 1993, pp. 124.
[6]   M. Sfakiotakis, D. M. Lane and J. B. C. Davies, "Review of Fish Swimming Modes for Aquatic Locomotion", IEEE Journal of Oceanic Engineering, Vol. 24, No. 2, April, 1999, pp.237-252.
[7]   Yong-Jai Park, Useok Jeong, et. al. "Kinematic condition for maximizing the thrust of a robotic fish using a compliant caudal fin", IEEE Transactions on Robotics, 10.1109/TRO。2012.2205490.
[8]   Junzhi Yu, Min Tan, etc., "Development of a biomimetic robotic fish and its control algorithm", IEEE Trans. on Systems, Man, and Cybernetics – part B: Cybernetics, Vol. 34, No.4, 2004, pp.1798-1810.
[9]   Z. L. Wang, G. R. Hang, J. Li, el. "A micro-robot fish with embedded SMA wire actuated flexible biomimetic fin", *Sensors and Actuators A: Physical*, Vol. 144, 2008, pp. 354-360.
[10] E. Mbemmo, Z. Chen, S. Shatara and X. B. Tan, "Modeling of Biomimetic Robotic Fish Propelled by an Ionic Polymer-Metal Composite Actuator", *2008 IEEE International Conference on Robotics and Automation*, Pasadena, CA, USA, May 19-23, 2008, pp.689-694.
[11] Z. Li, R. Du, M. C. Lei, S. M. Yuan, "Design and Analysis of a Biomimetic Wire-Driven Robot Arm," *Proceedings of the ASME 2011 International Mechanical Engineering Congress & Exposition*, IMECE2011, Denver, Colorado, USA, Nov. 11-17, 2011.
[12] Z. Li, R. Du, "Design and Analysis of a Biomimetic Wire-Driven Flapping Propeller", *2012 4th IEEE RAS & EMBS International Conference on Biomedical Robotics and Biomechatronics (BioRob)*, Jun. 24-27, Roma, Italy, pp.276-281.
[13] Z. Li, Wenqi Gao, R. Du and Baofeng Liao, "Design and Analysis of a Wire-Driven Robot Tadpole", Proceedings of the ASME 2012 International Mechanical Engineering Congress & Exposition (IMECE), Nov. 9-15, Houston, TX, USA. (No. IMECE2012-87462).
[14] Z. Li, R. Du and Yupei Yao, "Flying Octopus – A LTAV with Wire-Driven Flapping Wings", Proceedings of the ASME 2012 International Mechanical Engineering Congress & Exposition (IMECE), Nov. 9-15, Houston, TX, USA. (No. IMECE2012-87408).
[15] Nakashirna M, Ono K. "Development of a two-joint dolphin robot". Journal of Neurotechnology for biomimetic robots, 2002: 309.
[16] Yu J, Hu Y, Fan R, et al. "Mechanical design and motion control of a biomimetic robotic dolphin". Journal of Advanced Robotics, 2007, 21(3-4): 499-513.
[17] M. J. Lighthill, "Hydromechanics of aquatic animal propulsion", *Collected papers of Sir James Lighthill Volume IV*, Oxford University Press, 1997.
[18] M. J. Lighthill, "Note on the swimming of slender fish", *Journal of Fluid Mechanics*, Vol. 9, part 2, 1960, pp. 305-317.
[19] McCormick, Barnes W. "Aerodynamics, aeronautics and flight mechanics", pp. 24, John Wiley & Sons, Inc., New York.